MODELLING OF PATTERN FORMATION DURING THE MELTING OF SILICON BY HF EM FIELD

BERGFELDS K., VIRBULIS J., KRAUZE A.
Faculty of Physics and Mathematics, University of Latvia
8 Zeļļu str., LV-1002, Riga, Latvia
E-mail: kristaps.bergfelds@lu.lv

Abstract. The present work investigate causes of inhomogeneous silicon melting during floating-zone crystal growth. It is proposed that this phenomenon is caused by the concentration of electric current in the melt which is caused by the different material properties of silicon melt and solid. Coupled model of EM, temperature and phase change field is developed and used to describe the transient melting-solidification process. *Octave/Matlab* script language is used for the implementation of this model. Calculation results demonstrate that melt structure development is related to the magnetic skin-depth in solid silicon

1. Introduction

During floating-zone (FZ) crystal growth, high-frequency electromagnetic (HF EM) field is used to melt the polycrystalline silicon feed rod. Usually inductor current with a frequency around 3 MHz is used to ensure sufficiently small penetration depth of the EM field for proper melting of the feed rod [1]. In case of lower frequencies, instable shape of feed rod melting surface can develop [2].
However, even with 3 MHz inductor current, ring-like silicon melt structures parallel to the current lines are formed during the FZ process on the surface of the feed rod with radial size of 1-2 mm (Fig. 1, left). Similar non-homogenous melting occurs when 5 mm thick silicon plate is located under the HF inductor (Fig. 1, right). Resulting melt pattern can be used to determine the asymmetry of the inductor currents [3].

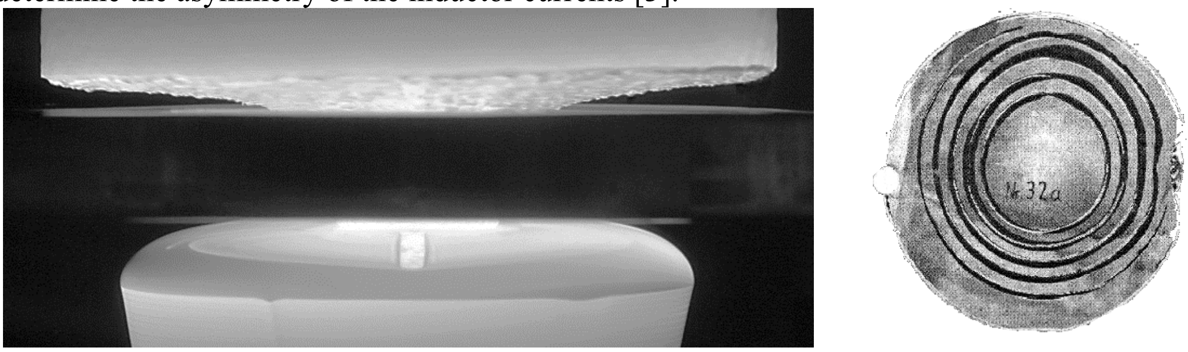

Figure 1: Left: inhomogeneous melting front on the feed-rod in a floating-zone silicon growth process [1]. Right: molten rings on a silicon plate created by HF EM inductor [3].

It is important to understand the formation of these structures as it is crucial to ensure continuous and stable melting during the FZ process. The ability to maintain stable growth at relatively low frequencies can even be regarded as key for growing larger diameter FZ crystals, i.e. larger melting powers can be achieved by lowering the frequency and thus inductor impedance [4]. Such motivation dictates that research regarding inhomogeneous melting during silicon HF EM melting is a worthwhile effort.

Melt pattern formation on silicon material has been studied previously – laser beam irradiation on a silicon surface creates ridges with size comparable to radiation wavelength and orientation determined by the beam polarization [5]. Such situation arises due to interference between incident beam and scattered radiation from surface imperfections. This example shows that periodic material structures are common result of non-linear system evolution. It is also clear that revealing the driving force of such pattern formation is a valuable contribution to the understanding of processes within such non-linear systems.

2. Mathematical model

Previously described problem is studied in a local scale. Two-dimensional domain of solid silicon with dimensions of 5×5 mm and orientation normal to direction of electric current is chosen (Fig. 2). It is believed to be small enough to assume homogenous boundary conditions, but sufficiently large for considered melt structures to develop. In this region temperature and phase change is calculated. In order to obtain EM induced heat sources, magnetic field is calculated in the silicon as well as in the air region between silicon and inductor surfaces. It is assumed that inductor is located 5 mm from the silicon surface. All calculations are carried out by using finite difference method implemented within *Octave/Matlab* environment.

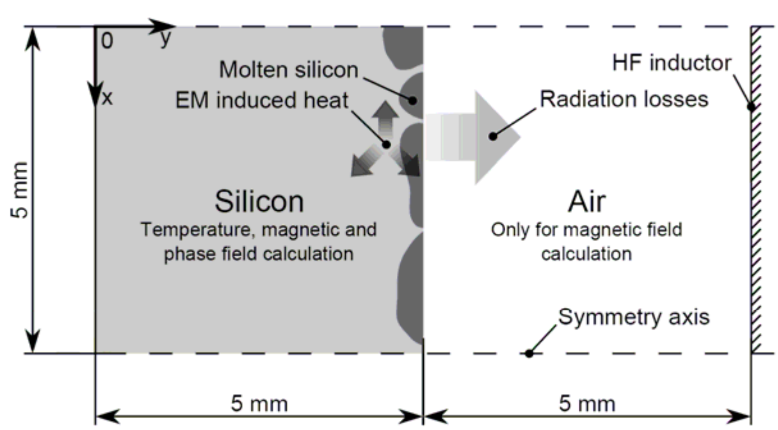

Figure 2: Schematics of the modelled system. Domain size and modelled physical processes are depicted.

Phase field model [6] is used to describe transient melting-solidification process. Assumption has been made that the phase transition happens within a narrow temperature interval ΔT_S. In such case the crystallization fraction f_c could be modeled as the temperature function (1).

$$f_c = \begin{cases} 0 & \text{if} \quad T > T_0 + \Delta T_S/2 \\ \dfrac{T_0 + \Delta T_S/2 - T}{\Delta T_S} & \text{if} \quad T \geq T_0 - \Delta T_S/2 \text{ and } T \leq T_0 + \Delta T_S/2 \\ 1 & \text{if} \quad T < T_0 - \Delta T_S/2 \end{cases} \tag{1}$$

With such assumption, the transient equation of conductive heat transfer can be written as (2). Insulation boundary conditions are used on the symmetry axis, fixed temperature value on the inside of the domain, but radiation condition on the surface with air.

$$\left(\rho c_p - L\frac{\mathrm{d}f_c}{\mathrm{d}T}\right)\frac{\partial T}{\partial t} = \lambda \Delta T + q_{EM} \tag{2}$$

EM induced heat sources q_{EM} are obtained by calculating the magnetic vector potential (3) which has only one non-zero component in the chosen system geometry. Zero-value boundary condition is used on the inside of silicon domain, but fixed-value condition on inductor surface is varied to account different inductor currents and thus melting powers.

$$\frac{\partial^2 A_z}{\partial x^2} + \frac{\partial^2 A_z}{\partial y^2} - i\omega\sigma\mu A_z = 0, \qquad q_{EM} = \frac{|-i\sigma\omega A_z|^2}{\sigma} \tag{3}$$

Material properties that are relevant to the developed mathematical model are listed in [7, 8]. These values are obtained by laboratory experiments and extensively used for mathematical modelling purposes. Electrical conductivities for melt $\sigma_m = 1.2 \cdot 10^6\ ^S/_m$ and solid

$\sigma_s = 5 \cdot 10^4$ S/m should be noted as important parameters regarding the investigated problem. Emissivity coefficient is modelled as temperature dependent parameter (Fig. 3, left).

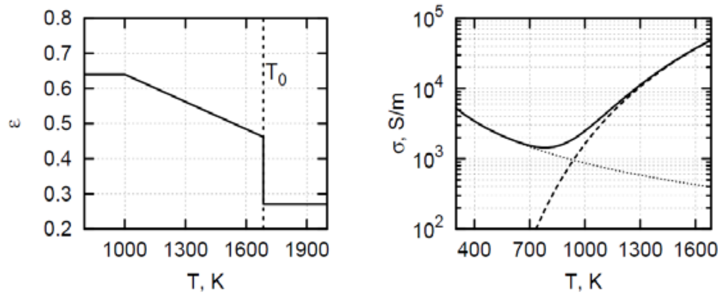

Figure 3: Left: modelled silicon emissivity coefficient temperature dependence. Right: modelled temperature dependence of solid silicon (solid line) as sum of conduction electron generation (dashed line) and conductivity due to dopants (dotted line).

When calculation studies involve large temperature intervals, temperature dependent heat conductivity of solid silicon is considered as suggested in [9]. Assumption is made that conductivity is determined of two processes – generation of conductivity electrons and presence of dopants in the material (Fig. 3, right).

3. Calculation results

Calculations were first carried out with a setup and mesh shown in Fig. 4. After 20 s stationary structure of melt regions with a size of about 1.4 mm were obtained for a certain simulated inductor current interval (Fig. 5). The magnetic field lines are bended in Si and gas and the induced heat sources are concentrated in molten regions.

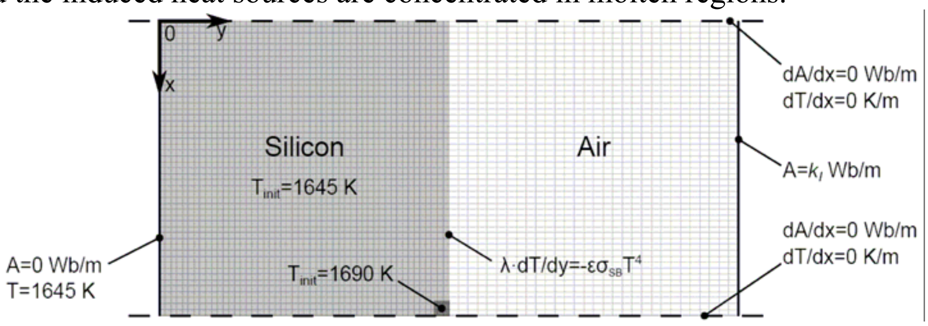

Figure 4: Schematics of the modelled system. Calculation mesh, initial and boundary conditions are displayed.

Such structures are obtained when initial temperature field perturbation is used. In case of uniform initial temperature field, completely uniform melting process occurs with no phase-field distribution variation along the direction of silicon surface. Further studies indicated that inhomogeneous vector potential boundary condition (linear distribution of 5–10% slope on 5 mm length) is also sufficient to obtain observed melt patterns.

Further studies considered different materials properties to locate the determinative parameters that ensure the melt pattern formation. Varied parameters were: solid silicon electrical conductivity, magnetic field frequency and emissivity coefficient of silicon melt.

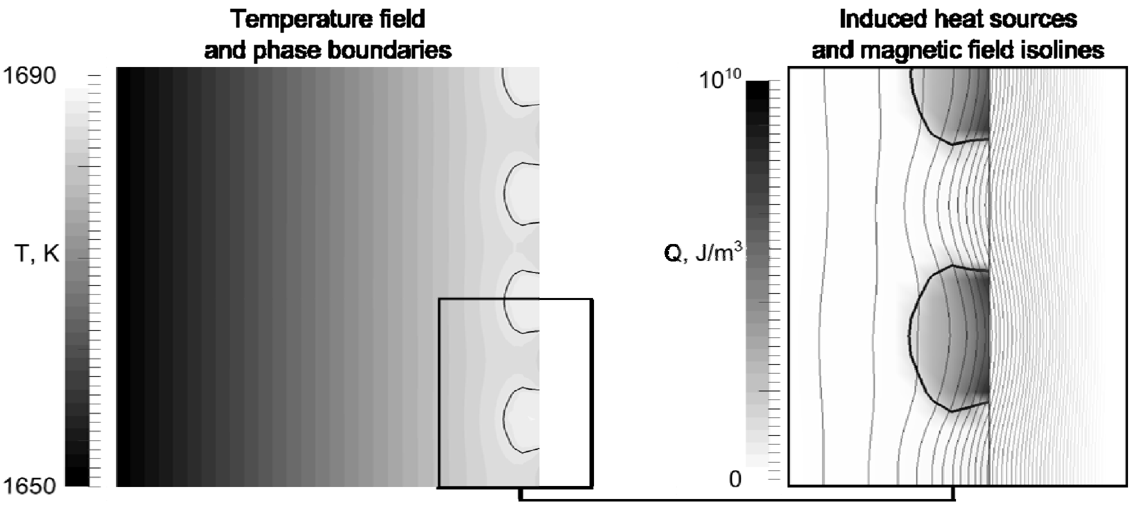

Figure 5: Calculation results for case with stationary melt structures developed during the course of 20 s treatment with HF EM field.

By applying equal and fixed value of 0.64 as emission coefficient of both melt and solid, it was observed that pattern formation still occurred. This proves that different emissivity properties of solid and liquid Si are not imperative for the observed phenomena. However, in this study solid silicon layer formed on top of melt regions due to comparatively larger radiative losses from the surface.

By varying the solid silicon conductivity, different spatial pattern distribution developed (Fig. 6, left). Additionally, EM field frequency variation causes similar effect. Such situation can be analyzed in a context of skin-depth $\delta = 1/\sqrt{\pi f \sigma \mu}$ (where f is frequency, σ is electrical conductivity, but μ is magnetic constant). Such approach illustrates the process characteristics at least qualitatively (Fig. 6, right). It must be noted that spatial pattern remained unchanged if different length of silicon surface l_x was used for calculations (blue and yellow lines in Fig. 6, right).

To simulate aforementioned practices with 5 mm thick Si plate under HF EM inductor, calculations using radiation boundary condition on both sided of silicon domain were performed. Additionally, initial temperature of 300 K were used in the domain (with 45 K perturbation at the corner) to simulate the effects of hugely varying electrical conductivity (as in Fig. 3, right). In this case non-stationary melt patterns were obtained at about 20% higher inductor powers as previous studies with fixed temperature boundary condition (Fig. 7). It must be noted that distance between observed melt regions is noticeably larger.

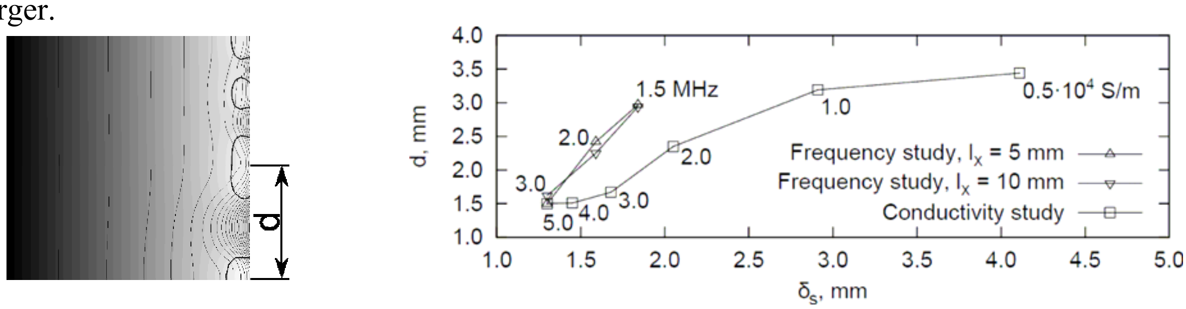

Figure 6: Left: Calculated temperature field, phase boundary (thick black line) and magnetic field at reduced electrical conductivity of $2 \cdot 10^4$ S/m. Right: melt region size as a function of skin-depth in solid silicon for calculation studies with various frequencies (triangular data points) and solid silicon electrical conductivities (rectangular data points).

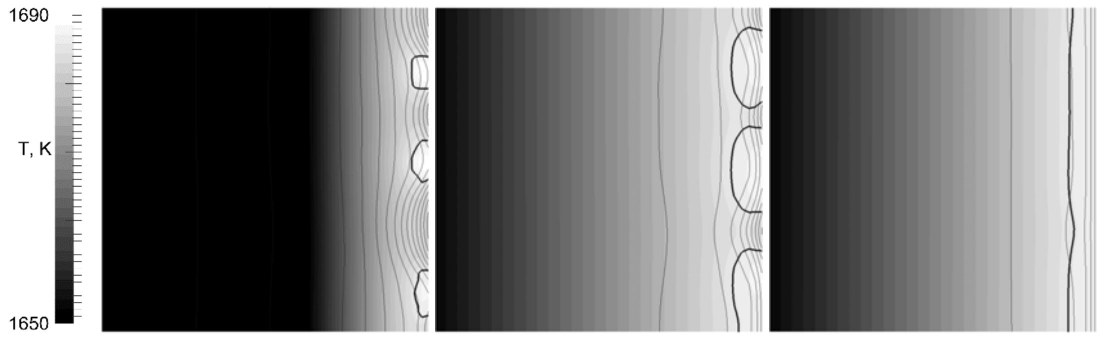

Figure 7: Calculated temperature field, phase boundary (thick black line) and magnetic field (thin black lines). From left to right: time instances of 3.5, 8.0 and 16.0 seconds.

4. Conclusions

Present work demonstrates that melt pattern formation during inductive melting of Si is determined by the EM field interaction with two-phase environment with different electrical conductivities. Characteristic size of patterns has been shown to be around 1.4 mm which corresponds well to observed situation in floating-zone furnaces. Wider structures are obtained at lower solid Si electrical conductivities which also correspond qualitatively to observations [3]. It has been shown that, in general, size of patterns is related to the skin-depth in the solid material and thermal boundary conditions.

5. Acknowledgements.

This work has been supported by the European Regional Development Fund, project Contract № 2013/0051/2DP/2.1.1.1.0/13/APIA/VIAA/009.

6. References

[1] T. Duffar, Crystal Growth Processes Based on Capillarity: Czochralski, Floating Zone, Shaping and Crucible Techniques, Wiley-Blackwell, 2010.

[2] W. Wünscher, A. Lüdge and H. Riemann, "Crucible-free pulling of germanium crystals," *Journal of Crystal Growth,* vol. 318, no. 1, pp. 1039-1042, 2011.

[3] H. Riemann, A. Ludge, K. Bottcher, H. J. Rost, B. Hallmann, W. Schroder, W. Hensel and B. Schleusener, "Silicon Floating Zone Process: Numerical Modeling of RF Field, Heat Transfer, Thermal Stress, and Experimental Proof for 4 Inch Crystals," *Journal of The Electrochemical Society,* vol. 142, no. 3, pp. 1007-1014, 1995.

[4] R. Menzel, "Growth Conditions for Large Diameter FZ Si Single Crystals," *Ph.D. Thesis at the Technische Universität Berlin,* 2013.

[5] J. F. Young, J. S. Preston, H. M. van Driel and J. E. Sipe, "Laser-induced periodic surface structure. II. Experiments on Ge, Si, Al, and brass," *Phys. Rev. B,* vol. 27, no. 2, pp. 1155-1172, 1983.

[6] I. Steinbach, M. Apel, T. Rettelbach and D. Franke, "Numerical simulations for silicon crystallization processes—examples from ingot and ribbon casting," *Solar Energy Materials and Solar Cells,* vol. 72, no. 1-4, pp. 59-68, 2002.

[7] A. Muhlbauer, A. Muiznieks, J. Virbulis, A. Ludge and H. Riemann, "Interface shape, heat transfer and fluid flow in the floating zone growth of large silicon crystals with the needle-eye technique," *Journal of Crystal Growth,* vol. 151, no. 1-2, pp. 66-79, 1995.

[8] A. Sabanskis, K. Bergfelds, A. Muiznieks, T. Schröck and A. Krauze, "Crystal shape 2D modeling for transient CZ silicon crystal growth," *Journal of Crystal Growth,* vol. 377, pp. 9-16, 2013.

[9] C. Kittel, Introduction to Solid State Physics, 8th ed., Wiley, 2005.